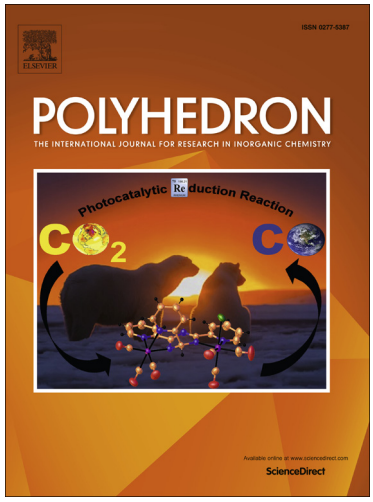

Niobium(V) peroxo α-amino acid complexes: synthesis, stability and kinetics of inhibition of acid phosphatase activity

Sandhya Rani Gogoi, Gangutri Saikia, Kabirun Ahmed, Rituparna Duarah, Nashreen S. Islam

PII: S0277-5387(16)30487-9
DOI: http://dx.doi.org/10.1016/j.poly.2016.09.057
Reference: POLY 12245

To appear in: *Polyhedron*

Received Date: 10 May 2016
Revised Date: 14 September 2016
Accepted Date: 28 September 2016

Please cite this article as: S. Rani Gogoi, G. Saikia, K. Ahmed, R. Duarah, N.S. Islam, Niobium(V) peroxo α-amino acid complexes: synthesis, stability and kinetics of inhibition of acid phosphatase activity, *Polyhedron* (2016), doi: http://dx.doi.org/10.1016/j.poly.2016.09.057

Niobium(V) peroxo α-amino acid complexes: synthesis, stability and kinetics of inhibition of acid phosphatase activity

Sandhya Rani Gogoi, Gangutri Saikia, Kabirun Ahmed, Rituparna Duarah and Nashreen S. Islam*

*To whom correspondence should be addressed:
Fax: +91-3712-267006
E-mail: nsi@tezu.ernet.in
nashreen.islam@rediffmail.com

Address: Prof. Nashreen S. Islam
Dept. of Chemical Sciences
Tezpur University
Napaam, Tezpur-784028
Assam, India

Phone : +91-9435380222 (Off.)
+91-3712-267007

Niobium(V) peroxo α-amino acid complexes: synthesis, stability and kinetics of inhibition of acid phosphatase activity

Sandhya Rani Gogoi, Gangutri Saikia, Kabirun Ahmed, Rituparna Duarah and Nashreen S. Islam*

Abstract

The present work was undertaken with an objective to investigate some biologically relevant attributes of peroxoniobium (pNb) derivatives, using a set of heteroleptic pNb compounds containing biogenic species as co-ligands. New peroxoniobium complexes corresponding to the general formula, $Na_2[Nb(O_2)_3L]$ (L=alanine or valine) were synthesized and comprehensively characterized by elemental analysis, IR, Raman, ^{13}C NMR, ^{1}H NMR, AAS and UV-Vis spectral studies, as well as thermogravimetric analysis. The structures of the compounds have been studied by density functional theory (DFT) method and their stability in solution at physiological pH has been ascertained. These compounds, along with our previously reported arginine and nicotinate complexes, $Na_2[Nb(O_2)_3(arg)]\cdot 2H_2O$ and $Na_2[Nb(O_2)_3(nic)(H_2O)]\cdot H_2O$, respectively were screened for their activities with two different types of enzymes *viz.,* catalase and acid phosphatase (ACP). Employing wheat thylakoid ACP as the model enzyme, it has been demonstrated for the first time that peroxoniobium derivatives serve as active inhibitors of phosphatase (IC_{50} values 2-9 μM). Enzyme kinetics data revealed that compounds exert mixed type of inhibition on ACP activity (Kii>Ki). Each of the tested pNb species exhibited significant resistance to degradation under the effect of catalase *vis-a-vis* the native substrate of the enzyme, H_2O_2.

Keywords: Peroxoniobium complex, ACP inhibition, Catalase resistance, Heteroleptic peroxoniobate

1. Introduction

The contemporary interest on peroxo compounds of niobium mainly originates from their utility as ideal water soluble precursors to obtain Nb-based oxide materials for high technology applications [1-3], in addition to their use as efficient and versatile oxidation catalysts [1,4-6]. It is intriguing to note that although Nb belongs to the same periodic group as vanadium, very few studies dealing with exploration of biochemical potential of peroxo compounds of niobium [7,8] are available in contrast to peroxovanadates (pV). Compounds of vanadium including the peroxovanadates have gained a special status in medicinal inorganic chemistry mainly as antineoplastic and insulin-mimetic agents [9-22], despite the fact that most of the synthetic pV compounds are unstable under physiological condition and are toxic [10,11,13,17]. It is notable that Nb has been known to be practically non-toxic to animals in comparison to vanadium [23]. Compounds of Nb have also been documented to exhibit anti-cancer activity [7,24] and niobium substituted heteropolytungstates were found to be potent anti-HIV-1 agents while being minimally cytotoxic [25]. According to a recent report, vanadate and niobate are strong inhibitors of the sarcoplasmic reticulum (SR) Ca^{2+}-ATPase that can affect calcium homeostasis, cell signalling, and many other cellular processes [26].

The process of enzyme inhibition has already been identified as an important pathway for action of inorganic drugs in recent years [27]. For instance, insulin-like activity of vanadium compounds has been linked to the inhibitory effect of V-compounds on phosphatases [28]. In fact, phosphohydrolases have become a key target for studying metabolism [29,30], for modifying cell signalling

[30,31,32] and for treatment of diseases owing to the pivotal role of phosphatases in signal transduction pathways [29,30,33]. The efficacy of vanadium based phosphatase inhibitors have been comprehensively reviewed by McLauchlan and co-workers recently [30], in which it has been observed that, notwithstanding the existence of numerous studies dealing with relative inhibitory potency such as EC_{50} of V as well as Mo and W derivatives, the reports in which mode of inhibition and *K*i values have been defined are still very limited. Surprisingly, no reports appear to exist so far, on *in vivo* or *in vitro* effect of discreet pNb complexes on phosphohydrolases. Pertinent here is to mention that we have previously investigated several bio-relevant aspects of peroxometallates [34-36] including detailed inhibition kinetics of phosphatases involving monomeric [37-39], dimeric [37,40] as well as macromolecular complexes of V, Mo and W [41-43]. In the present study, in continuation of our work on peroxometallates, we deemed it imperative to examine some of the heretofore unexplored biologically important features of pNb derivatives including their activity with phosphatase using wheat thylakoid membrane ACP as model enzyme. Apart from playing vital roles in diverse biological phenomena, these enzymes serve as excellent models to probe the metal induced inhibitory effect in membrane proteins [44-46].

We have also considered it important to study the effect of catalase, the enzyme responsible for the decomposition of H_2O_2 to H_2O and O_2 in the intercellular peroxisomes, on hetero as well as homoleptic pNb complexes. Hydrogen peroxide, being a reactive oxygen species (ROS) has long been known as a major contributor to DNA damage, protein oxidation and lipid peroxidation, which can ultimately lead to cell death [47-49]. In recent years however, the view that H_2O_2 is a toxic waste product has changed following the reports documenting

its importance as a key signal transducing agent which regulate a variety of cellular processes [20,21,35,50-52]. Rapid decomposition of cellular H_2O_2 by catalase and glutathione peroxidase has been found to be a hindrance for studying the cellular effects of H_2O_2 [20,21,35,50]. This has led to a search for peroxide derivatives that can substitute for H_2O_2, which would be less susceptible to degradation by catalase, yet efficient in their action. A fascinating finding of our previous studies has been the resistance exhibited by some of the metal bound peroxides towards degradation under catalase action [37-42]. Diperoxovanadate has already been recognized as a useful tool in studies of cellular effects mediated by H_2O_2 [35,50,53].

In this paper, we present the synthesis and characterization of two new members of heteroleptic pNb complexes with amino acids, alanine and valine as ancillary ligands. In nature, amino acids usually promote solubility of metals in aqueous environment and impart stability by complexation and increase their bioavailability. One of the factors believed to be responsible for the paucity of information related to biological studies of Nb compounds, is the restricted aqueous chemistry of the metal which is confined to very few available water soluble compounds [1,2,7,8,54-61]. We have recently gained an access to a pair of new triperoxoniobium complexes, $Na_2[Nb(O_2)_3(arg)]\cdot 2H_2O$ (arg = arginate) (**NbA**) and $Na_2[Nb(O_2)_3(nic)(H_2O)]\cdot H_2O$ (nic = nicotinate) (**NbN**) as auxiliary ligands which proved to be excellent catalysts for selective oxidation of thioethers with H_2O_2, in neat water [62]. Here, we report our findings on hydrolytic stability, steady state kinetic studies of the effect of the pNb complexes, **NbA**, **NbN**, **NbAla** and **NbVal** as well as the parent complex, $Na_3[Nb(O_2)_4]\cdot 13H_2O$ (**NaNb**) on acid phosphatase *in vitro*. Our results confirm that apart from being highly potent

inhibitors of the model enzyme, the compounds exhibit significant resistance to degradation under catalase action.

2. Experimental

2.1 Materials and methods

Niobium pentoxide, *p*-nitrophenyl phosphate (*p*-NPP), catalase, wheat thylakoid membrane acid phosphatase (ACP) used in this study were obtained from Sigma–Aldrich Chemical Co., Milwaukee, USA. Sodium thiosulphate, potassium hydrogen phosphate, potassium dihydrogen phosphate, citric acid, glacial acetic acid were purchased from Merck, India. L-alanine and L-valine were obtained from SRL, Mumbai, India and hydrogen peroxide (30%), sodium citrate (dihydrate) from Rankem, India.

The niobium content of the synthesized compounds was determined by atomic absorption spectroscopy (AAS) using Thermo iCE 3000 series atomic absorption spectrophotometer model analyst 200, as well as by gravimetric estimation [63]. Elemental analyses for C, H and N was performed on an elemental analyzer (Perkin-Elmer 2400 series II). Peroxide content for the compounds were determined, as has been described in earlier paper [64], by adding a weighed amount of the compound to a cold solution of 1.5% boric acid (w/v) in 0.7 M sulfuric acid (100 mL) and titration with a standard cerium (IV) solution. The sodium content was measured by AAS and also with an ionometer (Orion Versaster).

The IR spectra were recorded by making pressed pellets of samples with KBr using Perkin-Elmer spectrum 100 FTIR spectrophotometer. Raman spectra of the compounds were recorded using a Renishaw InVia Raman microscope equipped

with an argon ion laser with an excitation wavelength of 514 nm and a laser maximum output power of 20 mW. Thermogravimetric analysis (TGA) was carried out on a SHIMADZU TGA-50 system at a heating rate of 10 °C min^{-1} under N_2 atmosphere using an aluminium pan. ^1H NMR and ^{13}C NMR spectra with D_2O as solvent were recorded using a JEOL JNM-ECS400 spectrometer with the following parameters for ^{13}C NMR spectra: a carbon frequency of 100.5 MHz, 4096 X-resolution points, 1000-20000 number of scans, 1 s of acquisition time, and 30° pulse length. Cary model Bio 100 spectrophotometer equipped with a Peltier-controlled constant temperature cell was used for spectroscopic determinations of the initial rate of ACP catalyzed hydrolysis of *p*-NPP at 30 °C.

*2.2 $Na_3[Nb(O_2)_4]\cdot 13H_2O$ (**NaNb**) synthesis [6]*

The precursor complex, $Na_3[Nb(O_2)_4]\cdot 13H_2O$, was prepared by fusing 1 g of Nb_2O_5 with 1.85 g of NaOH in a nickel crucible at 700 °C, as has been reported previously. The solid product was cooled and subsequently dissolved in 100 mL of 1 M aqueous H_2O_2. Unreacted Nb_2O_5 was filtered off and the filtrate was allowed to stand at 5 °C for 24 h to obtain the crystals of $Na_3[Nb(O_2)_4]\cdot 13H_2O$.

*2.3 Synthesis of $Na_2[Nb(O_2)_3(Ala)]$, **NbAla** (Ala = L-alanine) and $Na_2[Nb(O_2)_3(Val)]$, **NbVal** (Val = L-valine)*

In a typical reaction, 0.6550 g (1.25 mmol) of solid sodium tetraperoxoniobate, $Na_3[Nb(O_2)_4]\cdot 13H_2O$ (**NaNb**) was dissolved in minimum volume (4 mL, 25 mmol) of 30% H_2O_2 in a 250 mL beaker. Maintaining the temperature of the reaction solution below 4 °C in an ice bath, the respective amino acid (1.25 mmol) was added gradually to it with constant stirring. The molar ratio of Nb: ligand was maintained at 1:1. The mixture was stirred for *ca.* 15 min till all

solid dissolved and a clear solution was obtained, which was subsequently allowed to stand for 3 h. The pH of the resultant solution was recorded to be *ca*. 6. On addition of pre-cooled acetone to the reaction solution with constant stirring, a white pasty product separated out which on repeated treatment with acetone under scratching turned into microcrystalline solid. The compound was separated by centrifugation and dried in *vacuo* over concentrated sulfuric acid.

The complexes, $Na_2[Nb(O_2)_3(arg)]\cdot 2H_2O$ (arg = arginate) (**NbA**) and $Na_2[Nb(O_2)_3(nic)(H_2O)]\cdot H_2O$ (nic = nicotinate) (**NbN**) were prepared according to procedures reported earlier [62].

2.4 Computational details

The Gaussian09 programme [65] at the B3LYP/LANL2DZ level of theory has been used to perform density functional theory (DFT) [66] calculations. The ground-state geometry of the two niobium complexes were obtained in the gas phase, and the minima of the optimized structures were verified by the absence of imaginary frequencies.

2.5 Stability of the complexes in aqueous solution

In order to assess the stability of the compounds in solution, a stock solution (100 mL) was prepared for each of the compounds maintaining the initial compound concentration as 0.2 mM, by adding weighed amount of the respective compound **NaNb** (0.105 mg/mL), **NbA** (0.089 mg/mL), **NbN** (0.079 mg/mL), **NbAla** (0.065 mg/mL) or **NbVal** (0.070 mg/mL). The peroxide content was then determined in aliquots drawn from the stock solution at different time intervals by the procedure described above under Section 2.1, for a period of 12 h. Stability of the compounds in solution at pH 4.6, pH 7.0 and 8.0, respectively, maintained by using phosphate buffer (50 mM, pH 4.6, pH 7.0 or 8.0), at pH 1.2 and 2.1 (50mM KCl/HCl buffer), and at pH 3.1 (50 mM citrate buffer) was similarly measured. Moreover, electronic, ^{1}H NMR

and ^{13}C NMR spectra of the compounds were monitored at 30 min time intervals for any possible change over a period of 12 h, as a measure of stability of the compounds in solution.

2.6 Effect of catalase on the pNb complexes

The extent of catalase induced decomposition of the compounds was evaluated by determining the change in peroxide content of the compounds in a solution consisting of the pNb compound in phosphate buffer and the enzyme, at specified time intervals as has been reported earlier [37-42]. The test solution containing the phosphate buffer (50 mM, pH 7.0) and catalase (40 μg/mL) was incubated at 30 ^{o}C. The volume of the test solution was kept at 100 mL. The weighed amount of the respective pNb compound as mentioned in **Table 6**, was then added to the test solution and aliquots of 5 mL were drawn out at an interval of 5 min from the starting of reaction and its peroxide content was determined after quenching the reaction by adding it to cold sulfuric acid (0.7 M, 100 mL).

2.7 Acid phosphatase activity

The acid phosphatase activity was assayed spectrophotometrically employing *p*-nitrophenyl phosphate (*p*-NPP) as a substrate [43,45,67,68]. In the standard assay, the reaction mixture contained acetate buffer (0.1 M, pH = 4.6), the enzyme (18.38 μg protein mL^{-1}) and different concentrations of pNb species (concentration varies between 1-12 μM, as shown in **Fig. 7** and **Fig. 8**) or the free ligand. The reaction was started by addition of the substrate *p*-NPP to the test solution which was pre-incubated for 5 min. After 30 min of incubation of the reaction solution at 30 ^{o}C, the reaction was terminated by addition of 0.9 mL of 0.5 M NaOH solution and the absorbance at 405 nm was recorded in order to determine the *p*-NP produced (molar extinction coefficient of the *p*-nitrophenolate = 18000 M^{-1} cm^{-1})

[69]. The enzyme activity in the absence of the inhibitors was determined which was used as the control. The half-maximal inhibitory concentration of the inhibitor species giving 50% inhibition (IC_{50}) was determined graphically. All experiments were performed in triplicate. The data in the figures are presented as the means ± SE from three separate experiments.

2.8 Determination of the kinetic constants

The kinetic constants, maximum velocity (*V*max*)* and Michaelis constant (*K*m*)* were determined from Lineweaver–Burk plots following a rearrangement of the Michaelis–Menten equation [68,70,71] using Cary 100 Bio Enzyme Kinetics software.

$$\frac{1}{V} = \left\{ \frac{K_m}{V_{\max}[S]} + \frac{1}{V_{\max}} \right\}$$

In the present case, the following equation was used to characterize the mode of inhibition, which was found to be of mixed type:

$$V = \left\{ \frac{V_{\max} \times [S]}{K_m\left(\frac{1+[I]}{K_i}\right) + [S]\left(\frac{1+[I]}{K_{ii}}\right)} \right\}$$

where *V* is the velocity, [*S*] is the *p*-NPP concentration and [*I*] denotes the inhibitor concentration, *K*i and *K*ii are inhibitory constants for the competitive part and non competitive part, respectively. The enzyme inhibitor constants were determined from secondary plots of the initial rate data by a linear regression analysis. In order to obtain *K*i, the slopes from the Lineweaver plots were re-plotted against the inhibitor concentration values from the x-intercepts of these re-plots. The *K*ii was

obtained from the plot of intercepts that has been found from the Lineweaver plots against the inhibitor concentration values from the x-intercepts of these re-plots.

3. Results and Discussions

3.1 Synthesis and characterization

The white microcrystalline pNb compounds, $Na_2[Nb(O_2)_3(Ala)]$ **(NbAla)** and $Na_2[Nb(O_2)_3(Val)]$ **(NbVal)** were obtained by stabilizing peroxoniobium species in a ligand sphere of L-alanine or L-valine in presence of excess H_2O_2. Water soluble precursor complex, $Na_3[Nb(O_2)_4]\cdot 13H_20$, used as the source of niobium, has been prepared by the literature method [6]. The maintenance of pH of *ca.* 6 and limiting the amount of water to that contributed by 30% H_2O_2 appeared to be the key parameters responsible for the successful synthesis of the compounds in an aqueous medium. The near neutral pH apparently favoured the formation of the triperoxoNb species and co-ordination of the amino acids in their anionic form, facilitating the synthesis of the desired complexes. It is pertinent to mention that ligands with carboxylate functional group have been identified as excellent co-ligands for stabilizing peroxoNb(V) species [1,8,54-61].

From the elemental analysis data (**Table 1**), the ratio of Nb: O_2^{2-} content in the title complexes was found to be 1:3 whereas, the C, H, N analysis results indicated the Nb: amino acids ratio as 1:1 in each of them. The values are consistent with the

<Table 1>

formation of triperoxoniobium species with one amino acid co-ligand in the co-ordination sphere and are in accord with their formulation as $Na_2[Nb(O_2)_3L]$ (L= alanine or valine). Occurrence of Nb in its +5 oxidation state in the

synthesized compounds has been confirmed from the magnetic susceptibility measurements, which showed the compounds to be diamagnetic.

3.2 IR, Raman and electronic spectral studies

The IR and Raman spectra of the compounds **NbAla** and **NbVal** displayed sufficiently well resolved spectral patterns main features of which are summarized in **Table 2**. The spectra of both **NbAla** and **NbVal** (**Fig. 1**) exhibited three bands in the 850-800 cm^{-1} region, which are typical of ν(O-O) modes of η^2-peroxo groups belonging to a triperoxoniobium species [1,72]. The presence of three side-on

<Table 2>

bound peroxo groups in the complexes has been corroborated further by the complementary Raman spectra. The $\nu_{as}(Nb\text{-}O_2)$ and $\nu_s(Nb\text{-}O_2)$ absorptions were observed in the expected 500-600 cm^{-1} region, respectively in the IR as well as Raman spectra [1,73].

<Fig. 1>

Presence of co-ordinated amino acids in the complexes was also evident from their IR and Raman spectra which displayed characteristic shifts in the positions of the vibrations attributable to amino acids, relative to the corresponding free ligand values. The assignments were made on the basis of relevant literature data [74-79]. The free alanine spectrum exhibited $\nu_{as}(COO^-)$ and $\nu_s(COO^-)$ vibrations at 1586 and 1409 cm^{-1}, respectively with a frequency difference $\Delta\nu$ = 177 cm^{-1} [$\Delta\nu = \nu_{as}(COO^-) - \nu_s(COO^-)$]. In case of free valine, these bands were located at 1570 and 1395 cm^{-1}. A definite shift of $\nu_{as}(COO^-)$ to a higher frequency and that of $\nu_s(COO^-)$ to a lower frequency (**Table 2**) and the resulting frequency difference of 266 and 234

cm^{-1} found in **NbAla** and **NbVal**, respectively are typical of unidentately co-ordinated non-protonated carboxylate groups (**Table 2**) [74,75].

The participation of amino groups of the ligands in co-ordination was indicated by the shift of *v*(NH) frequencies to a lower wave number in comparison to the free amino acid bands. The well-resolved medium intensity band observed in the spectra of **NbAla** at 3081 cm^{-1} and the two bands occurring at 3058 and 3162 cm^{-1} for **NbVal** have been ascribed to the NH stretchings of co-ordinated amino acid [74]. The $\delta(NH_2)$ vibrations appeared at *ca.* 1510 cm^{-1} in the spectra of both the complexes. A band at 490 cm^{-1} has been observed in the free alanine zwitterion for NH_3^+ torsion [78]. On complexation, the peak disappeared and additional peaks have been obtained at 477 and 411 cm^{-1} in the IR spectrum of **NbAla** which may be assigned to ν_{as}(Nb-N) and ν_s(Nb-N) stretchings, respectively [74]. Similarly, the presence of 430 and 405 cm^{-1} peaks owing to ν_{as}(Nb-N) and ν_s(Nb-N) stretchings in the spectrum of **NbVal** constitutes an additional valuable indication for the involvement of NH_2 group in coordination [74]. The intense peak observed between 2980-2880 cm^{-1} in the Raman spectra occurring as a medium intensity peak in the IR spectra of both the complexes have been assigned to C-H stretching vibration.

The electronic spectra of complexes **NbAla** and **NbVal** displayed a broad absorption between 300 and 350 nm which is characteristic of peroxo to metal charge transfer transition of peroxo derivatives of niobium [7,59,61,62].

3.3 ^1H and ^{13}C NMR studies

The ^1H NMR spectra for the pNb complexes **NbVal** and **NbAla** in D_2O are presented in **Fig. 2** and **Fig. S1** (Supplementary Information), respectively and the

corresponding chemical shifts for the complexes and free amino acids are listed in **Table 3**. A close resemblance was observed in the ^{1}H NMR spectra of the complexes and the spectra of the respective amino acid displaying the well-resolved resonances with expected integration and peak multiplicities. The spectra

<Fig. 2>

however, showed distinct up field shift of the proton signals attached to carbon atoms C-2 and C-3 relative to the free ligand, consistent with the occurrence of metal ligand co-ordination [62,80,81]. Similar upfield shift of the proton signals have been observed earlier in case of arginine containing complex **NbA** [62] as well, which appears to be common feature among the reported metal compounds containing co-ordinated amino acids [80-82]. The position of H-4 and H-5 protons in **NbVal** remains practically unaffected which may not be unexpected as these atoms are well-separated from the actual ligand donor sites.

<Table 3>

The ^{13}C NMR spectra of ligands L-alanine and L-valine exhibited resonances due to the carboxylate carbon atoms at 175.81 and 174.24 ppm, respectively, apart from the expected peaks corresponding to the side chain carbon atoms [80]. As seen in **Fig. S2** (Supplementary Information) and **Table 4,** all the signals appear with downfield shift to varying degrees, *vis-a-vis* the free amino acids, obviously

<Table 4>

resulting from the deshielding of carbon atoms as a consequence of complexation [41,62,80]. The most significant co-ordination induced shift $\Delta\delta$ ($\delta_{\text{complex}} - \delta_{\text{free carboxylate}}$) ≈ 7.02 ppm for **NbAla** (8.55 ppm for **NbVal**) occurred as expected for

the metal linked carboxylate carbon, suggesting a strong metal-ligand interaction [41]. Appearance of carboxylate carbon resonance as a single peak in the spectra of the compounds reflected a single carbon environment for co-ordinated carboxylate [41]. Thus, in conformity with the ^{1}H NMR evidence, ^{13}C NMR spectra too, testify to the presence of only one complex species in solution confirming that the compounds did not hydrolyze and remained intact in solution. Thus apart from valuable structural information, the NMR analysis data provided persuasive evidence in support of the stability of the compounds in solution.

3.4 TGA-DTG analysis

The TGA-DTG plots [**Fig. 3 (a)** and **(b)**] obtained for the title compounds on heating up to a temperature of 700 ^{o}C, revealed a close analogy among their decomposition patterns. Each of the compounds, as has been observed in case of previously reported complexes, **NbAla** and **NbVal** undergoes continuous degradation and do not explode on heating [55,59,62,83-85]. A significant common feature shared by the two pNb compounds, as evident from the respective thermograms, is the absence of water molecule in the compounds.

<Fig. 3>

Although existence of homo- or heteroleptic pNb complexes without free or bound water molecule is not unprecedented [1,54,83,86,87], majority of heteroligand pNb complexes including the ones reported previously by us (**NbA** and **NbN**) [62], and sodium tetraperoxoniobate, **NaNb** [6] contain either outer sphere or co-ordinated, or both types of water molecules [1,54,55,59,83]. The first decomposition stage occurs in **NbAla** and **NbVal** in the temperature ranges of 135-210 °C and 140-205 °C, respectively attributable to loss of co-ordinated peroxo

groups from the complexes. Subsequently, ligand degradation takes place in the temperature range of 243-480 °C in case of **NbAla** (241-389 °C for **NbVal**) and further continues up to a final decomposition temperature of 700 °C. The residue remaining from the pNb compounds after their complete degradation was characterized to be oxoniobate species. The IR spectra of the residue showed the characteristic *v*(Nb=O) absorptions and complete disappearance of the signature peaks pertaining to peroxo as well as amino acids of the original compounds. The TGA-DTG analysis data for the compounds thus furnished further endorsement in support of the composition and formula assigned to the compounds.

Taking into account the above collective evidences the structure of the complex ions may be represented by eight co-ordinated polyhedra of the type shown in **Fig. 4**, comprising of three terminal peroxo groups and an amino acid occurring as a bidentate ligand, bonded to Nb(V) *via* carboxylate and amino groups.

<Fig. 4>

3.5 Theoretical investigation

The viability of the proposed structures for the complexes, **NbAla** and **NbVal** was further supported by the results of density functional theory (DFT) [66] calculations at the B3LYP/LANL2DZ level of theory. The initial structures of the two complexes were modelled on the basis of the experimentally derived structural information. Presented in **Fig. 5** are the optimized geometries of the niobium

<Fig. 5>

complexes which show coordination spheres of the two complexes comprising of central metal atom (Nb) surrounded by three η^2-peroxo groups and deprotonated amino acid ligand bonded *via* O(carboxylate) and N(amino) atoms. While one of the peroxo groups occupies a *trans* position to the co-ligand, the other two are in *cis* configuration. The coordination polyhedron around the niobium atom in each of the complexes is a dodecahedron which is in accord with the structures of majority of the reported pNb complexes [1,59], including the ones studied herein *viz.,* **NbA** and **NbN** [62]. Moreover, the geometrical parameters such as the bond angles and bond lengths obtained from DFT calculations (**Table 5**) are within the range typical of the heteroleptic peroxoniobium(V) complexes. The bond distances associated with the peroxo groups *viz.,* Nb-O and O-O bonds vary between 2.023 to 2.086 Å and 1.552 to 1.557 Å, respectively. The geometrical parameters derived from the theoretical calculations are in close agreement with the reported crystallographic data obtained for other triperoxoniobium(V) complexes consisting of N,O-donor ligands in the co-ordination sphere [1,6,54-61].

<Table 5>

We have also calculated vibrational frequencies for the optimized geometries of the pNb compounds **NbAla** and **NbVal**. The theoretically obtained IR and Raman data presented in **Table 2,** correlated well with the respective experimentally determined frequencies. The small deviations observed between the calculated and experimental spectral data appear to be within the acceptable limit and are not unusual as the calculated spectral data were obtained from gas phase optimized geometries of the complexes. The reported average error for frequencies calculated with the B3LYP functional was of the order 40-50 cm^{-1} for inorganic molecules [88]. Thus the results of our theoretical studies substantiate the

experimental observations and impart additional validity to the proposed geometries for the complexes **NbAla** and **NbVal**.

3.6 Stability of the complexes toward decomposition in solution

We have examined the stability of the pNb compounds in solution under varying pH conditions **(Fig. 6)**. Compound stability was verified with respect to loss of co-ordinated peroxo groups by determining the peroxide content and monitoring the electronic spectra for any possible change at specified time intervals. In addition to pH of 9-10 which is the natural pH of the synthesized pNb

<Fig. 6>

compounds in solution, the stability was tested at pH values ranging from 1.2 to 8.0. We found that neither peroxide content of the compounds under investigation nor the position or intensity of their electronic spectral absorptions undergo any significant change during a period of 12 h. Furthermore, ^{13}C and ^{1}H NMR spectra of the pNb compounds when monitored over a period of 12 h remained practically unaltered **(Fig. 2)**. These results are mutually consistent and collectively corroborate that the compounds retain their solid state structure in solution.

3.7 Interaction of pNb compounds with catalase

The effect of catalase on the hetero-ligand pNb complexes **NbA, NbN, NbAla** and **NbVal**, as well as the parent complex, **NaNb** are shown in **Fig**. **6.** The data presented in **Table 6** demonstrate that in presence catalase at pH 7, each of the heteroligand pNb compounds undergoes gradual degradation with loss of peroxide.

<Table 6>

On the other hand, addition of catalase to a 0.1 mM solution of its native substrate, H_2O_2 leads to rapid degradation of H_2O_2 with release of half equivalent of oxygen (molecular basis) with a rate of 430 μM/min as expected from the disproportionation reaction, and the process is completed within *ca.* 2 min [53]. This difference in rates of degradation between H_2O_2 and the pNb species indicates that the compounds are at least 30-50 fold weaker as substrate to the enzyme, with respect to H_2O_2. From the above results it may be surmised that co-ordination of peroxo ligand to Nb enhances its resistance towards degradation under catalase action. It is also notable that the initial rates of degradation of the tested pNb compounds vary from compound to compound (**Table 6**) suggesting that the ability of the complexes to withstand catalase action is influenced by the auxiliary ligand environment. On comparing these values with those obtained from some of the previously reported monomeric hetero-ligand peroxo complexes of d^0 metal ions *viz.,* V and Mo, it emerged that peroxo groups attached to Nb show comparable degree of resistance with respect to pV compounds [37-42] whereas, these are several fold more resistant to catalase action than the molybdenum containing analogues [41].

On the basis of the peroxo groups present in these complexes, total peroxide loss was expected to be 0.6 mM for the triperoxo compounds and 0.8 mM for tetraperoxo compound from a solution of 0.2 mM compound concentration. We have previously observed that the catalase action on compounds of V, Mo and W led to nearly complete loss of their peroxide content within *ca.* 30 min of incubation as anticipated [37-42]. In contrast, as seen in **Fig. 6** in case of the pNb complexes, after the initial loss of two molecules of peroxo groups of the triperoxoNb complexes, within *ca.* 30 min of incubation, a unique feature observed

for each of the pNb complexes is that, the compounds continued to retain one molecule of peroxide even beyond a period of *ca.* 1 h. The formation of a monoperoxo species of Nb and its high resistance to catalase action is thus evident from our data.

It is pertinent to mention that, we have preferred to employ phosphate buffer in the present study, as the use of near neutral phosphate buffers has proven to be most satisfactory in several previous investigations dealing with peroxovanadates [41,53,89,90] as well as peroxo compounds of Mo(VI) and W(VI) [41,43], studied in our laboratory. Although vanadate has been reported to react with most of the compounds used in buffer including phosphate [89,91], pV compounds are known to be fairly inert and do not react with non-reducing buffers such as phosphate [53,89,90]. It is important to note that we have also conducted similar experiments using Hepes as buffer in lieu of phosphate buffer (**Fig. S3** and **Fig. S4**, Supplementary Information). The rates of catalase induced degradation of the pNb compounds derived from these experiments showed no significant variation (17.0, 11.0, 9.4 and 11.9 μM/min for **NaNb**, **NbA**, **NbN** and **NbVal,** respectively) from the results obtained using phosphate buffer (**Table 6**), suggesting that these buffer systems have no observable influence on the stability or the degradation profile of the compounds in solution, under the employed experimental condition.

3.8 Inhibitory effect of pNb compounds on acid phosphatase

We have investigated the inhibitory mechanism of the pNb complexes on ACP activity *in vitro*. The phosphatase inhibitory effect of the triperoxoniobium compounds *viz.,* **NbA, NbN, NbAla** and **NbVal**, as well as the parent tetraperoxoniobate, **NaNb** upon activity of the wheat thylakoid membrane ACP

was evaluated employing standard enzyme assay system and *p*-NPP as substrate. A variety of enzyme assays have been made use of previously, to measure phosphatase inhibition by metal compounds such as vanadates, molybdates and tungstates [30,41,43,45,68,71]. The mode of enzyme inhibition such as competitive, non-competitive or mixed type can usually be ascertained [92] by varying the inhibitor concentration and measuring the enzyme activity at various substrate concentrations. The findings of our investigation on dose response inhibition of the model enzyme activity by the pNb complexes are illustrated in **Fig. 7.** The inhibitor potential of the test compounds was quantified in terms of the half-maximal inhibitory concentration (IC_{50}). The IC_{50} values recorded, being within the range of 2-9 μM, implied that the compounds are highly potent inhibitors of the enzyme (**Fig. 7, Table 7**). While the IC_{50} value of tetraperoxo species was observed to be comparable to that displayed by triperoxoNb complexes with arginine (**NbA)** and nicotinic acid (**NbN)** as co-ligands, the compounds **NbVal** and **NbAla** was found to be relatively less potent. Since individually the free ligands had no observable effect on the enzyme activity, under the employed assay conditions, the above observations indicate that the inhibitory

<Fig. 7>

effect of the pNb compounds indeed originate from the interaction of the intact metal complexes with the enzyme and the ligand environment influences the inhibitor potency of the tested intact complexes.

<Table 7>

To establish the mechanism of inhibition for the acid phosphatase catalyzed hydrolysis of *p*-NPP by the inhibitor species, the steady state kinetics of this

process were investigated and kinetic parameters *K*m and *V*max were determined [68,70,71]. The L-B plots of the reciprocal initial velocity versus the reciprocal substrate concentration in the absence and presence of the inhibitor complexes at various concentrations are shown in **Fig. 8 (**for **NaNb, NbN** and **NbAla)** and **Fig. S5** [(for **NbA** and **NbVal)** (Supplementary Information)]. Kinetic measurements yielded straight lines with point of intersection in the second quadrant in each case. As can be readily seen in **Fig. 8** as well as in **Fig. S5** (Supplementary Information)**,** both *V*max and *K*m values are affected by the presence of each of the inhibitors showing an increase in *K*m and decrease in velocity *V*max values with increasing inhibitor concentration. This behaviour is characteristic of mixed type of inhibition combining competitive and non-competitive modes. We have also determined the inhibitor constants K_i and K_{ii}

<Fig. 8>

in order to assess the affinity of the enzyme for the inhibitors. The inhibitor constant K_i is a measure of the affinity of the inhibitor for the free enzyme whereas, K_{ii} reflects its affinity for the enzyme-substrate complex. The ratio of K_{ii} and K_i values were used to assess the relative competitiveness of each inhibitor. A larger K_{ii}/K_i value indicates a mixed type of inhibition that is relatively more competitive in its action, whereas a lower K_{ii}/K_i reflects the mixed type of inhibition that is more uncompetitive. On the other hand, when $K_{ii} = K_i$, the mode of inhibition becomes noncompetitive. In the present study, as shown in the inset to **Fig. 8** and **Fig. S5** (Supplementary Information), the inhibitor constant *K*i for the competitive part of inhibition, was obtained from the secondary plot of the slope of the primary plot ($1/V$ versus $1/[S]$) against the inhibitor concentration with the intercept on the inhibitor axis being -*K*i. The value of *K*ii, inhibitor constant for

non-competitive inhibition, was obtained from the replot of slope versus inhibitor concentration, with the inhibitor axis intercept being equivalent to -*K*ii. The kinetic results presented in **Table 7** show that for each of the inhibitors *K*ii > *K*i, confirming that pNb species exert mixed type of inhibition on ACP activity.

A competitive inhibitor is known to share a close structural resemblance to the natural substrate of the enzyme whereas, a non-competitive inhibitor binds reversibly at a site far removed from the active site causing a conformational change in the overall three-dimensional shape of the enzyme [43]. Acid phosphatases, isolated from various plant and animal sources, contain dinuclear iron active sites and highly conserved amino acid sequences with a histidine residue at the active site [44,45,93-96]. Although, oxy anions of V, Mo and W having penta or hexa co-ordinated structures have mostly been known to be competitive inhibitors of phosphatases due to their structural analogy with phosphate, however with respect to inhibition of acid phosphatases, different oxometallates have been shown to display different mechanistic preferences ranging from competitive, non-competitive to uncompetitive patterns of inhibition [43,97-100]. The work of Averill and co-workers demonstrated that oxyanions such as molybdate and tungstate being relatively larger in size, bind in a non-competitive fashion by bridging the two iron atoms in the binuclear active site of mammalian ACP, while the smaller anions may also bind at a single iron atom in a competitive manner [93]. Oxidative interaction between the highly oxidative compounds with the Fe^{2+} centre resulting in its oxidation to ferric form and consequent inactivation of the enzyme in a non-competitive manner was suggested as an additional possibility of inhibitory effect of these complexes [93]. In view of these observations as well as our findings on efficient oxidising ability displayed

by the test compounds [62], it is reasonable to expect that in the present study too, a similar mechanism involving oxidation of Fe^{2+} centre by the pNb species is perhaps operative, contributing to their mixed type of inhibition of ACP function, combining competitive and non-competitive pathways. However, in absence of direct evidence and due to the complicated chemistry and intricacy of the interactions between pNb species and complex biomolecules involved in the present study, it is difficult to comment on the exact mechanism of inhibition at this stage. Nevertheless, there are ample evidences in the literature highlighting the importance of redox properties of pV compounds in inhibition of protein phosphatases [28,101] which lend credence to our hypothesis.

4. Conclusions

The present work afforded a set of water soluble pNb complexes which contain species familiar to biological environment as co-ligand. The spectral and chemical data obtained have provided satisfactory evidences for the composition of the ligand sphere and the likely mode of ligation to the Nb(V) centre, which has been substantiated by the results of DFT calculations performed on the complexes. Our experiments confirm that the pNb complexes tested, induce strong inhibitory effect on acid phosphatase. Detailed inhibition kinetics studies clearly demonstrated that each of the compounds is a potent mixed-type of inhibitor of the enzyme, combining competitive and non-competitive modes of inhibition. The remarkable stability of the compounds in aqueous solution of a wide range of pH values, their ability to partially retain the coordinated peroxo groups even beyond 1 h of incubation with the ROS mopping enzyme catalase, are other distinctive attributes of the compounds.

Acknowledgements

Financial support from the Department of Biotechnology, New Delhi, India, is gratefully acknowledged. We are thankful to Dr. K. K. Bania, Department of Chemical Sciences, Tezpur University, for help in theoretical investigation and Dr. Gayatri Ramakishna, Cancer Biology Laboratory, Centre for DNA Fingerprinting and Diagnostics (CDFD), Hyderabad for valuable discussion. We are grateful to the Council of Scientific and Industrial Research (CSIR), New Delhi, India for providing Senior Research Fellowship to S.R.G.

References

[1] D. Bayot, M. Devillers, Coord. Chem. Rev. 250 (2006) 2610-2626.

[2] G. Stavber, B. Malic, M. Kosec, Green Chem. 13 (2011) 1303-1310.

[3] E. R. Leite, C. Vila, J. Bettini, E. Longo, J. Phys. Chem. B. 110 (2006) 18088-18090.

[4] H. Egami, T. Oguma, T. Katsuki, J. Am. Chem. Soc. 132 (2010) 5886-5895.

[5] H. Egami, T. Katsuki, Angew. Chem. Int. Ed. 47 (2008) 5171-5174.

[6] L. C. Passoni, M. R. H. Siddiqui, A. Steiner, I. V. Kozhevnikov, J. Mol. Catal. A: Chem. 153 (2000) 103-108.

[7] H. Thomadaki, A. Lymberopoulou-Karaliota, A. Maniatakou, A. Scorilas, J. Inorg. Biochem. 105 (2011) 155-163.

[8] A. Maniatakou, S. Karaliota, M. Mavri, C. Raptopoulou, A. Terzis, A. Karaliota, J. Inorg. Biochem. 103 (2009) 859-868.

[9] C. Djordjevic, G. L. Wampler, J. Inorg. Biochem. 25 (1985) 51-55.

[10] D. C. Crans, Vanadium compounds Chemistry, Biochemistry and Therapeutic Application. A. S. Tracey, D. C. Crans Oxford University Press, New York, 1998, pp. 60-71.

[11] C. Djordjevic, N. Vuletic, M. L. Renslo, B. C. Puryear, R. Alimard, Mol. Cell. Biochem. 153 (1995) 25-29.

[12] A. S. Tracey, G. R. Willsky, E. S. Takeuchi, Vanadium: Chemistry, Biochemistry, Pharmacology and Practical Application. CRC Press and Taylor & Francis Group: Boca Raton, 2007.

[13] M. Jelikic-Stankov, S. Uskokokovic-Markovic, I. Holclajtner-Antunovic, M. Todorovic, P. Djurdjevic, J. Trace Elem. Med. Biol. 21 (2007) 8-16.

[14] H. J. Thompson, N. D. Chasteen, L. D. Meeker, Carcinogenesis 5 (1984) 849-851.

[15] N. Butenko, A. I. Tomaz, O. Nouri, E. Escribano, V. Moreno, S. Gama, V. Rebeiro, J. P. Telo, J. Costa Pessoa, I. Cavaco, J. Inorg. Biochem. 103 (2009) 622-632.

[16] C. E. Heyliger, A. G. Tahiliani, J. H. Mcneill, Science 227 (1985) 1474-1477.

[17] K. H. Thompson, J. H. Mcneill, C. Orvig, Chem. Rev. 99 (1999) 2561-2572.

[18] Y. Shechter, I. Goldwaser, M. Mironchik, M. Fridkin, D. Gefel, Coord. Chem. Rev. 237 (2003) 3-11.

[19] B. I. Posner, R. Faure, J. W. Burgess, A. P. Bevan, D. Lachance, G. Zhang-Sun, I. G. Fantus, J. B. Ng, D. A. Hall, B. S. Lum, A. Shaver, J. Biol. Chem. 269 (1994) 4596-4604.

[20] T. Ramasarma, In Vanadium Biochemistry, M. A. Alves Ed. Research Signpost: India, 2007, pp 45-76.

[21] T. Ramasarma, Proc. Indian Natn. Acad. Sci. B69 (2003) 649-672.

[22] K. H. Thompson, J. Lichter, C. LeBel, M. C. Scaife, J. H. Mcneill, C. Orvig, Inorg. Biochem. 103 (2009) 554-558.

[23] K. Rydzynski, D. Pakulska, Patty's Industrial Hygiene and Toxicology, John Wiley & Sons Press, 2012.

[24] G. S. Kim, D. A. Judd, C. L. Hill, R. F. Schinazi, J. Med. Chem. 37 (1994) 816-820.

[25] P. Kopf-Maier, M. Leitner, H. Kopf, J. Inorg. Nucl. Chem. 42 (1980) 1789-1791.

[26] G. Fraqueza, C. Andre Ohlin, W. H. Casey, M. Aureliano, J. Inorg. Biochem. 107 (2012) 82-89.

[27] A. Y. Louie, T. J. Meade, Chem. Rev. 99 (1999) 2711-2734.

[28] D. C. Crans, J. J. Smee, E. Gaidamauskas, L. Yang, Chem. Rev. 104 (2004) 849-902.

[29] A.R. Saltiel, Cell 104 (2001) 517-529.

[30] C. C. McLauchlana, B. J. Petersb, G. R. Willsky, D. C. Crans, Coord. Chem. Rev. 301-302 (2015) 163-199.

[31] T. Hunter, Cell 80 (1995) 225-236.

[32] T. Hunter, Cell 100 (2000) 113-127.

[33] J. L. McConnell, B.E. Wadzinski, Mol. Pharmacol. 75 (2009) 1249-1261.

[34] A. K. Haldar, S. Banerjee, K. Naskar, D. Kalita, N. S. Islam, S. Roy, Exp. Parasitol. 122 (2009) 145-154.

[35] N. Chatterjee, S. Kiran, B. M. Ram, N. S. Islam, T. Ramasarma, G. Ramakrishna, Mech. Ageing Dev. 132 (2011) 230-239.

[36] A. Misra, S.Srivastava, S. R. Ankireddy, N. S. Islam, T. Chandra, A. Kumar, M. K. Barthwal, M. Dikshit, Redox Rep. 18 (5) (2013) 174-185.

[37] P. Hazarika, D. Kalita, N. S. Islam, J. Enzyme Inhib. Med. Chem. 23 (2008) 504-513.

[38] P. Hazarika, S. Sarmah, D. Kalita, N. S. Islam, Transit. Metal Chem. 33 (2008) 69-77.

[39] D. Kalita, S. P. Das, N. S. Islam, Biol. Trace Elem. Res. 128 (2009) 200-219.

[40] P. Hazarika, D. Kalita, S. Sarmah, N. S. Islam, Mol. Cell Biochem. 284 (2006) 39-47.

[41] J. J. Boruah, D. Kalita, S. P. Das, S. Paul, N. S. Islam, Inorg. Chem. 50 (2011) 8046-8062.

[42] D. Kalita, S. Sarmah, S. P. Das, D. Baishya, A. Patowary, S. Baruah, N. S. Islam, React. Funct. Polym. 68 (2008) 876-890.

[43] S. P. Das, S. R. Ankireddy, J. J. Boruah, N. S. Islam, RSC Advances 2 (2012) 7248-7261.

[44] D. E. Wilcox, Chem. Rev. 96 (1996) 2435-2458.

[45] M.-J. Fei, J.-S. Chen, X.-Y. Wang, J. Integr. Plant Biol. 48 (2006) 294-299.

[46] W. N. Lipscomb, N. Strater, Chem. Rev. 96 (1996) 2375-2433.

[47] S. Bhattacharjee, Current Sci. 89 (2005) 1113-1121.

[48] G. W. Winston, Free radicals in cells. In Stress Responses in Plants: Adaptation and Acclimation Mechanisms, Willy-Liss Inc, 1990, pp 57-86.

[49] C. H. Foyer, Oxygen metabolism and electron transport in photosynthesis, In Molecular Biology of Free Radical Scavenging Enzymes (ed. J. Scandalios), Cold Spring Harbor Laboratory, New York, 1997.

[50] M. Giorgio, M. Trinei, E. Migliaccio, P. G. Pelicci, Nat. Rev. Mol. Cell Biol. 8 (2007) 722-728.

[51] B. J. Goldstein, M. Kalyankar, X. Wu, Diabetes 54 (2005) 311-321.

[52] B. Chance, H. Sies, A. Boveris, Physiol. Rev. 59 (1979) 527-605.

[53] H. N. Ravishankar, A. V. S. Rao, T. Ramasarma, Arch. Biochem. Biophys. 321 (1995) 477-484.

[54] D. Bayot, B. Tinant, B. Mathieu, J.-P. Declercq, M. Devillers, Eur. J. Inorg. Chem. (2003) 737-743.

[55] D. Bayot, B. Tinant, M. Devillers, Inorg. Chem. 43 (2004) 5999-6005.

[56] D. Bayot, M. Degand, M. Devillers, J. Solid State Chem. 178 (2005) 2635-2642.

[57] D. Bayot, B. Tinant, M. Devillers, Inorg. Chem. 44 (2005) 1554-1562.

[58] D. Bayot, M. Degand, B. Tinant, M. Devillers, Inorg. Chim. Acta 359 (2006) 1390-1394.

[59] A. Maniatakou, C. Makedonas, C. A. Mitsopoulou, C. Raptopoulou, I. Rizopoulou, A. Terzis, A. Karaliota, Polyhedron 27 (2008) 3398-3408.

[60] A. C. Dengel, W. P. Griffith, Polyhedron 8 (1989) 1371-1377.

[61] Y. Narendar, G. L. Messing, Chem. Mater. 9 (1997) 580-587.

[62] S. R. Gogoi, J. J. Boruah, G. Sengupta, G. Saikia, K. Ahmed, K. K. Bania, N. S. Islam, Catal. Sci. Technol. 5 (2015) 595-610.

[63] A. K. Majumdar, A. K. Mukherjee, Anal. Chim. Acta 21 (1959) 245-247.

[64] M. K. Chaudhuri, S. K. Ghosh, N. S. Islam, Inorg. Chem. 24 (1985) 2706-2707.

[65] M. C. Frisch *et al.,* Gaussian 09, Revision A.1, Gaussian, Inc., Wallingford, CT, 2009; Gaussian 09, Revision A.1, M. J. Frisch, G. W. Trucks, H. B. Schlegel, G. E. Scuseria, M. A. Robb, J. R. Cheeseman, G. Scalmani, V. Barone, B. Mennucci, G. A. Petersson, H. Nakatsuji, M. Caricato, X. Li, H. P. Hratchian, A. F. Izmaylov, J. Bloino, G. Zheng, J. L. Sonnenberg, M. Hada, M. Ehara, K. Toyota, R. Fukuda, J. Hasegawa, M. Ishida, T. Nakajima, Y. Honda, O. Kitao, H. Nakai, T. Vreven, J. A. Montgomery Jr., J. E. Peralta, F. Ogliaro, M. Bearpark, J. J. Heyd, E. Brothers, K. N. Kudin, V. N. Staroverov, R. Kobayashi, J. Normand, K. Raghavachari, A. Rendell, J. C. Burant, S. S. Iyengar, J. Tomasi, M. Cossi, N. Rega, J. M. Millam, M. Klene, J. E. Knox, J. B. Cross, V. Bakken, C. Adamo, J. Jaramillo, R. Gomperts, R. E. Stratmann, O. Yazyev, A. J. Austin, R. Cammi, C. Pomelli, J. W. Ochterski, R. L. Martin, K. Morokuma, V. G. Zakrzewski, G. A.

Voth, P. Salvador, J. J. Dannenberg, S. Dapprich, A. D. Daniels, O. Farkas, J. B. Foresman, J. V. Ortiz, J. Cioslowski, D. J. Fox. Gaussian, Inc., Wallingford CT, 2009.

[66] R. G. Parr, W. Yang, Density Functional Theory of Atoms and Molecules, Oxford University Press, Oxford, 1989.

[67] R. Albrecht, J. L. Petit, V. Calvert, G. Terrom, C. Périssol, Bioresour. Technol. 101 (2010) 228-233.

[68] H. U. Bergmeyer, J. Bergmeyer and M. Grassl, Methods of Enzymatic Analysis, third ed., Weinheim, Deerfield Beach, FL, Verlag Chemie, 1983.

[69] C. V. Ferreira, E. M. Taga, H. Aoyama, Plant Sci. 147 (1999) 49-54.

[70] H. Lineweaver, D. Burk, J. Am. Chem. Soc. 56 (3) (1934) 658-666.

[71] A. Cornish-Bowden, Perspect. Sci. 1 (2014) 7-87.

[72] D. Bayot, M. Devillers, D. Peeters, Eur. J. Inorg. Chem. (2005) 4118-4123.

[73] W. P. Griffith, J. Chem. Soc. (1964) 5248-5252.

[74] K. Nakamoto, Infrared and Raman Spectra of Inorganic and Co-ordination Compounds, Part B, fifth ed., Wiley and Sons, New York, 1997.

[75] G. B. Deacon, R. J. Phillips, Coord. Chem. Rev. 33 (1980) 227-250.

[76] S. Kumar, Elixir Vib. Spec. 39 (2011) 4996-4999

[77] A. W. Herlinger, S. L. Wenhold, T. V. Long, J. Am. Chem. Soc. (1970) 6474-6481.

[78] S. T. Chow, C. A. Mcauliffe, J. Inorg. Nucl. Chem. 37 (1975) 1059-1064.

[79] C. A. McAulifte (1965) Thesis M S. Florida State University.

[80] M. A. Girasolo, S. Rubino, P. Portanova, G. Calvaruso, G. Ruisi, G. Stocco, J. Organomet. Chem. 695 (2010) 609-618.

[81] M. Nath, R. Yadav, G. Eng, P. Musingarimi, Appl. Organomet. Chem. 13 (1999) 29-37.

[82] E. M. A. Ratilla, B. K. Scott, M. S. Moxness, N. M. Kostie, Inorg. Chem. 29 (1990) 918-926.

[83] D. Bayot, B. Tinant, M. Devillers, Catal. Today 78 (2003) 439-447.

[84] J. K. Ghosh, G. V. Jere, Thermochim. Acta 136 (1988) 73-80.

[85] G. V. Jere, L. Surendra, M. K. Gupta, Thermochim. Acta 63 (1983) 229-236.

[86] C. W. Balke, E. F. Smith, J. Am. Chem. Soc. 30 (1908) 1637-1668.

[87] B. Cage, A. Weekley, L. C. Brunel, N. S. Dalal, Anal. Chem. 71 (1999) 1951-1957.

[88] I. Bytheway, M. W. Wong, Chem. Phys. Lett. 282 (1998) 219-226.

[89] A. Shaver, J. B. Ng, D. A. Hall, B. I. Posner, Mol. Cell Biochem. 153 (1995) 5-15.

[90] S. Sarmah D. Kalita, P. Hazarika, R. Borah, N. S. Islam, Polyhedron 23 (2004) 1097-1107.

[91] D. C. Crans, Comments Inorg. Chem. 16 (1994) 1-33.

[92] I. H. Segel, Enzyme Kinetics: Behavior and Analysis of Rapid Equilibrium and Steady State Enzyme Systems, Wiley, New York, 1975.

[93] J. B. Vincent, M. W. Crowder, B. A. Averill, Biochem. 30 (1991) 3025-3034.

[94] J. Shabanowitz, N.-Z. Zhu, T. Zirino, B. A. Averill, S. T. Daurat-Larroque, J. G. Shewale, R. M. Roberts, K. Brew, Biochem. Biophys. Res. Commun. 144 (1987) 1154-1160.

[95] C. M. Ketcham, R. M. Roberts, R. C. M. Simmen, H. S. Nick, J. Biol. Chem. 264 (1989) 557-563.

[96] D. K. Lord, N. C. P. Cross, M. A. Bevilacgua, S. H. Rider, P. A. Gorman, A. V. Groves, D. W. Moss, D. Sheer, T. M. Cox, Eur. J. Biochem. 189 (1990) 287-293.

[97] P. J. Stankiewicz, M. J. Gresser, Biochem. 27 (1988) 206-212.

[98] Y. S. Heo, J. M. Ryu, S. M. Park, J. H. Park, H. C. Lee, K. Y. Hwang, J. Kim, Exp. Mol. Med. 34 (2002) 211-223.

[99] R. L. Van-Etten, P. P. Waymack, D. M. Rehkop, J. Am. Chem. Soc. 96 (1974) 6782-6785.

[100] G. Soman, Y. C. Chang, D. J. Graves, Biochem. 22 (1983) 4994-5000.

[101] D. C. Crans, Peroxo, hydroxylamido, and acac derived vanadium complexes: chemistry, biochemistry and insulin mimetic action of selected vanadium compounds. In: A. S. Tracey, D. C. Crans (eds) Vanadium compounds chemistry, biochemistry, and therapeutic applications, Oxford University Press, New York, 1998, pp 82-103.

Captions for Figures

Fig. 1 (a) IR & (b) Raman spectra of NbAla and (c) IR & (d) Raman spectra of NbVal.

Fig. 2 The ^{1}H NMR spectra of NbVal in D_2O. The spectra were recorded as follows: (a) NbVal in D_2O immediately after preparation, (b) solution of (a) 12 h later.

Fig. 3 TGA-DTG plots of (a) NbAla and (b) NbVal.

Fig. 4 Peroxo compounds of Nb(V) under investigation in the current study. (A) Proposed structures of (a) **NbAla** and (b) **NbVal**. (B) Structures of (a) **NbA [62]**, (b) **NbN [62]** and (c) **NaNb [6]**.

Fig. 5 Optimized geometry of (a) NbAla and (b) NbVal. The numerical numbers represent the labeling of the atoms as in Table 5.

Fig. 6 Stability of compound **NaNb** at different pH values: (▲) compound solution in distilled water, pH of the solution = 10.0, (×) solution of complexes in phosphate buffer (50 mM, pH 7.0). Stability of compound **NbA** at different pH values: (●) compound solution in distilled water, pH of the solution = 9.0, (✶) solution of complexes in phosphate buffer (50 mM, pH 7.0). Effect of catalase on (♦) **NaNb**, (■) **NbA**, (**+**) **NbN**, (**-**) **NbAla** and (Δ) **NbVal.** The test solution contained phosphate buffer (50 mM, pH 7.0) and the catalase (40 μg/mL) which was incubated at 30 ^{o}C for 5 min. Compounds were then added to the reaction solution, aliquots were drawn at indicated time points, and loss in peroxide content was determined.

Fig. 7 The effect of (♦) NaNb, (▲) NbA, (×) NbN, (✶) NbAla, (●) NbVal and (■) free ligand on the activity of ACP. The ACP catalyzed rates of hydrolysis of *p*-NPP at pH 4.6 were determined at 30 ^{o}C by measuring A_{405} in a reaction mixture

containing ACP (18.38 μg mL^{-1}) and *p*-NPP (2 mM) in acetate buffer (0.1 M, pH = 4.6) in the absence or presence of stated concentrations of the inhibitors (for NaNb, NbA, NbN and the respective free ligand, compound concentrations: 1, 2, 3, 4 and 5 μM and for NbAla, NbVal and the respective free ligand, compound concentration: 2, 4, 6, 8, 10 and 12 μM). The data are presented as the means ±SE from three separate experiments.

Fig. 8 Lineweaver–Burk plots for the inhibition of ACP activity in the absence and presence of (A) NaNb, (B) NbN and (C) NbAla.The inset represents the secondary plot of the initial kinetic data of the Lineweaver plot. The reaction mixture contained acetate buffer (0.1 M, pH 4.6) and *p*-NPP (50-300 μM). The reaction was started by adding ACP (18.38 μg mL^{-1}) to the reaction solution, which was pre-incubated for 5 min and the rate of hydrolysis in the presence of ♦ 0 μM, ■ 2.5 μM, ▲5μM, × 7.5 μM, ✳ 10 μM inhibitors were obtained. The values are expressed as the mean ± SE from three separate experiments.

Inset: (a) the slopes were plotted against inhibitor concentrations and *K*i values were obtained from the x-intercepts of these re-plots. (b) The vertical intercepts were plotted against the inhibitor concentration and *K*ii values were obtained from the x-intercepts of these re-plots.

Table 1 Analytical data for the synthesized peroxo–niobium complexes

Compounds	% found from elemental analysis (Theoretical %)					% O_2^{2-} content	Ratio of
	C	H	N	Nb[a]	Na	(Theoretical %)	Nb:O_2^{2-}
$Na_2[Nb(O_2)_3(Ala)]$	11.03	1.84	4.28	28.59	14.19	29.42	
	(11.15)	(1.86)	(4.33)	(28.77)	(14.25)	(29.72)	1:2.97
$Na_2[Nb(O_2)_3(Val)]$	17.23	2.87	4.01	26.37	13.19	27.31	
	(17.10)	(2.85)	(3.99)	(26.48)	(13.11)	(27.36)	1:3.04

[a] Determined by AAS

Table 2 Experimental and theoretical infrared and Raman spectral data (cm^{-1}) for the **NbAla** and **NbVal** compounds

Assignement			**NbAla**	**NbVal**
ν(O-O)	IR	Exp.	849 (m), 825 (sh), 812(s)	846(m), 827(sh), 813(s)
		Calc.	864, 823, 811	858, 775
	R	Exp.	868 (sh), 845 (s), 826 (sh)	889 (sh), 845 (s), 827(sh)
		Calc.	872, 824	878, 851, 815
ν_s(Nb-O_2)	IR	Exp.	546 (s)	548 (s)
		Calc.	550	544
	R	Exp.	537 (s)	536 (s)
		Calc.	551	528
ν_{as}(Nb-O_2)	IR	Exp.	592 (m)	594 (m)
		Calc.	692	651
	R	Exp.	645 (sh)	684 (sh)
		Calc.	692	678
ν_{as}(COO^-)	IR	Exp.	1628 (s)	1586 (s)
		Calc.	1666	1601
	R	Exp.	1619 (vw)	1629 (vw)
		Calc.	1665	1600
ν_s(COO^-)	IR	Exp.	1362 (m)	1352 (m)
		Calc.	1405	1310
	R	Exp.	1414 (vw)	1393 (vw)
		Calc.	1388	1369

s, strong; m, medium; vw, very weak; sh, shoulder.

Table 3 ^{1}H NMR chemical shifts for ligands and heteroligand peroxo–niobate complexes

Compound	Chemical Shift (ppm)[a]			
	H-2	H-3	H-4	H-5
Alanine	3.68	1.35		
NbAla	3.62	1.33		
Valine	3.48	2.15	0.93	0.88
NbVal	3.46	2.14	0.93	0.88

[a] See **Fig. 4A** for the atomic numbering.

Table 4 ^{13}C NMR chemical shift for ligands and triperoxoniobium complexes, **NbAla** and **NbVal**

Compound	Carboxylate Carbon	Chemical Shift (ppm)[a]			
		C_2	C_3	C_4	C_5
Alanine	175.81	50.55	16.19		
NbAla	182.83	51.26	19.50		
Valine	174.24	60.34	29.07	17.96	16.63
NbVal	182.79	61.84	31.67	19.02	16.75

[a] See **Fig. 4A** for the atomic numbering.

Table 5 Selected bond lengths (Å) and bond angles (degree) for the two complexes calculated at the B3LYP/LANL2DZ level of theory

Structural index	**NbAla**	Structural index	**NbVal**
Nb-O2	2.062	Nb-O2	2.042
Nb-O3	2.059	Nb-O3	2.038
Nb-O4	2.029	Nb-O4	2.032
Nb-O5	2.024	Nb-O5	2.041
Nb-O6	2.042	Nb-O6	2.076
Nb-O7	2.086	Nb-O7	2.023
Nb-O8	2.225	Nb-O8	2.392
Nb-N9	2.394	Nb-N9	2.331
C10-O8	1.311	C10-O8	1.295
C10-O11	1.274	C10-O11	1.281
C12-N9	1.473	C12-N9	1.486
C12-C13	1.542	C12-C3	1.551
		C13-C14	1.546
		C14-C15	1.546
O2–O3	1.552	O2–O3	1.553
O4–O5	1.557	O4–O5	1.556
O6–O7	1.549	O6–O7	1.547
∠O2–Nb–O3	44.01	∠O2–Nb–O3	43.01
∠O4–Nb–O5	45.18	∠O4–Nb–O5	44.58
∠O6–Nb–O7	44.26	∠O6–Nb–O7	44.75
∠O8–Nb–N9	70.32	∠O8–Nb–N9	66.94

[a] See **Fig. 4A** for the atomic numbering.

Table 6 Catalase-dependent oxygen release from niobiumperoxo compounds

Compound	Concentration		Peroxide content (mM)	Loss of peroxide (μM/min)
	mg/mL	(mM)		
NaNb	0.105	0.2	0.8	16.7
NbA	0.089	0.2	0.6	11.4
NbN	0.079	0.2	0.6	8.6
NbAla	0.065	0.2	0.6	9.1
NbVal	0.070	0.2	0.6	11.6
DPV[a]	0.034	0.2	0.4	12.0
DMo_1[a*]	0.054	0.2	0.4	37.6

[a] Reference 41, [*] Amount of catalase = 10 μg/mL.

Table 7 Half-maximal inhibitory concentration (IC_{50}) and inhibitor constants (*K*i and *K*ii) values for pNb compounds

Compound	IC_{50} (μM)	*K*i (μM)	*K*ii (μM)	*K*ii/*K*i	Types of inhibition
NaNb	2.24	2.75	12.85	4.67	Mixed inhibition
NbA	2.59	2.70	7.10	2.63	Mixed inhibition
NbN	2.35	2.45	22.90	9.35	Mixed inhibition
NbAla	8.85	3.15	22.20	7.05	Mixed inhibition
NbVal	5.65	5.60	32.45	5.79	Mixed inhibition

[a] Note: the ACP catalyzed rates of hydrolysis of *p*-NPP at pH 4.6 were determined at 30 °C by measuring A_{405} in a reaction mixture containing ACP (18.38 μg mL^{-1}) and *p*-NPP (50-300 μM) in acetate buffer (0.1 M, pH = 4.6) in the presence of stated concentrations of the inhibitors (as shown in **Fig. 7** and **Fig. 8**).

Fig. 1

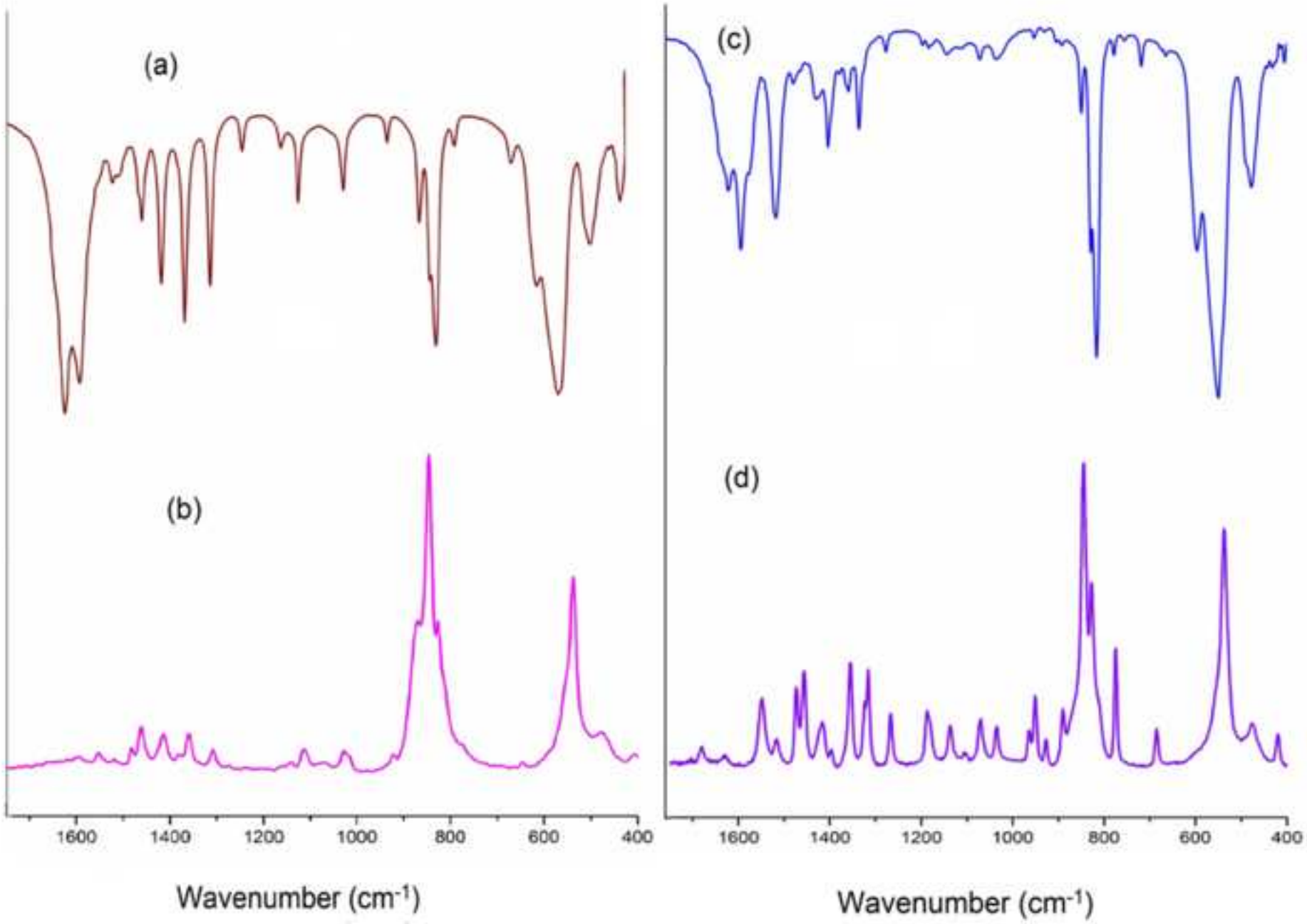

Fig. 2

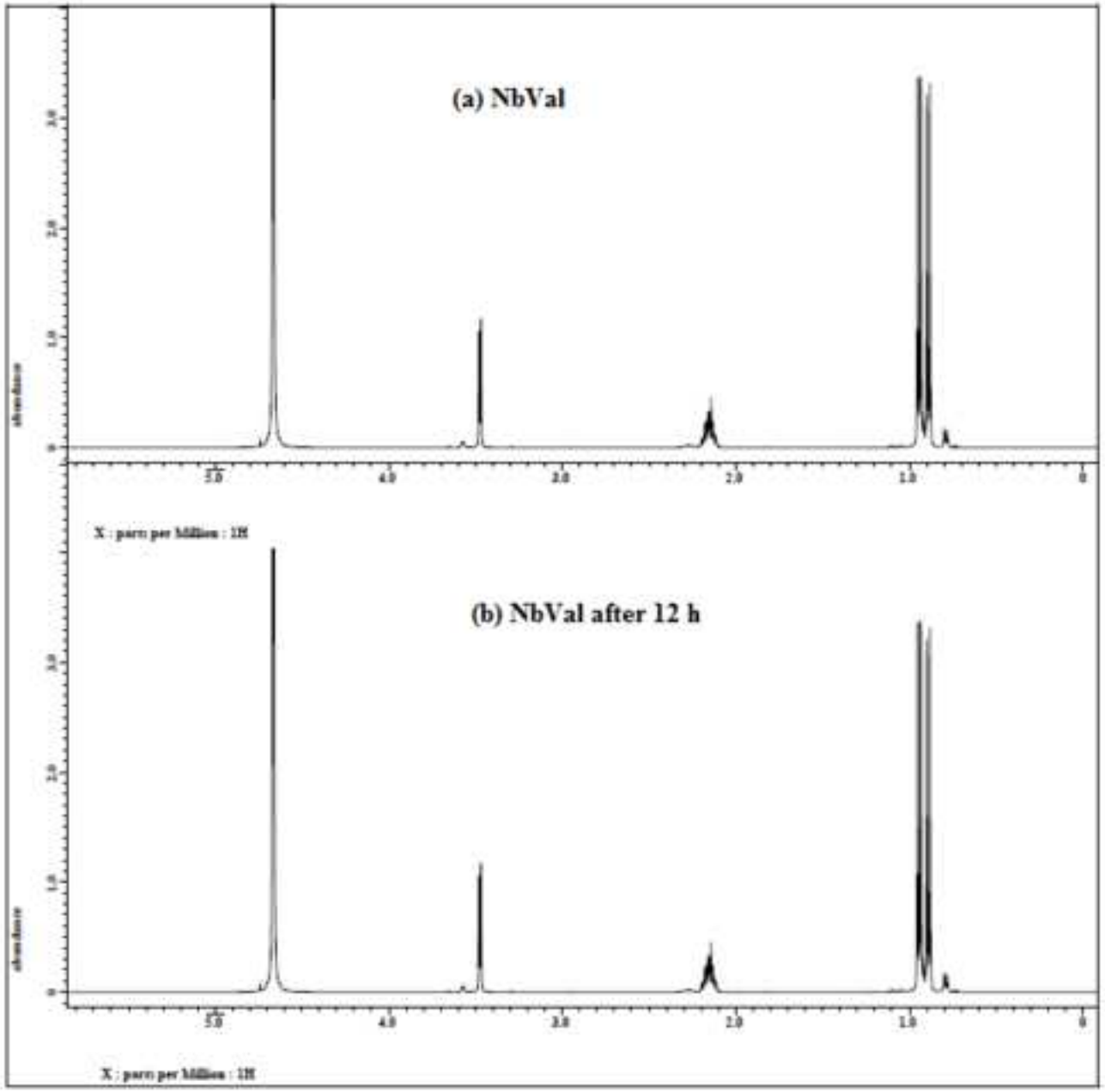

Fig. 3

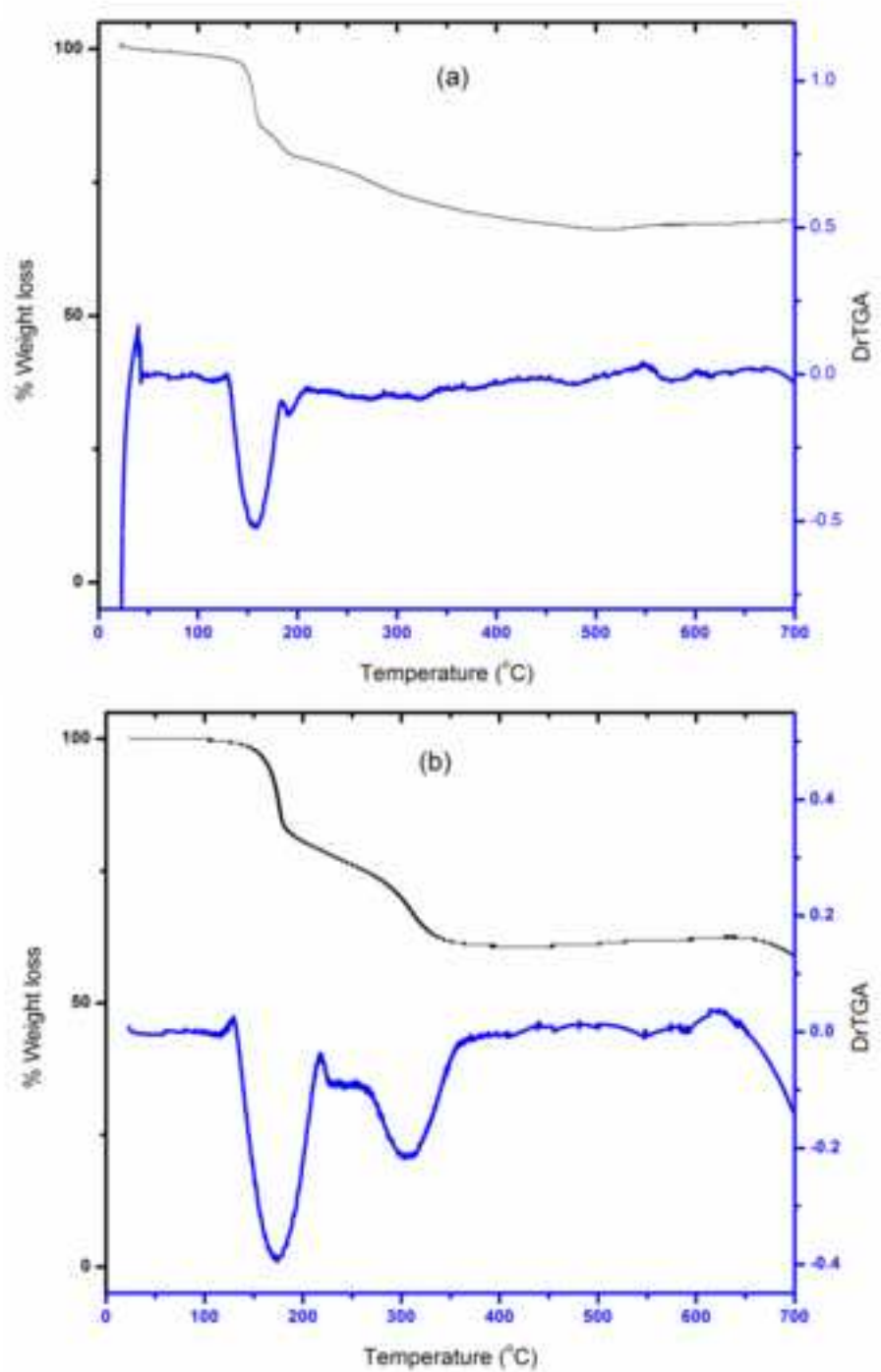

Fig. 4

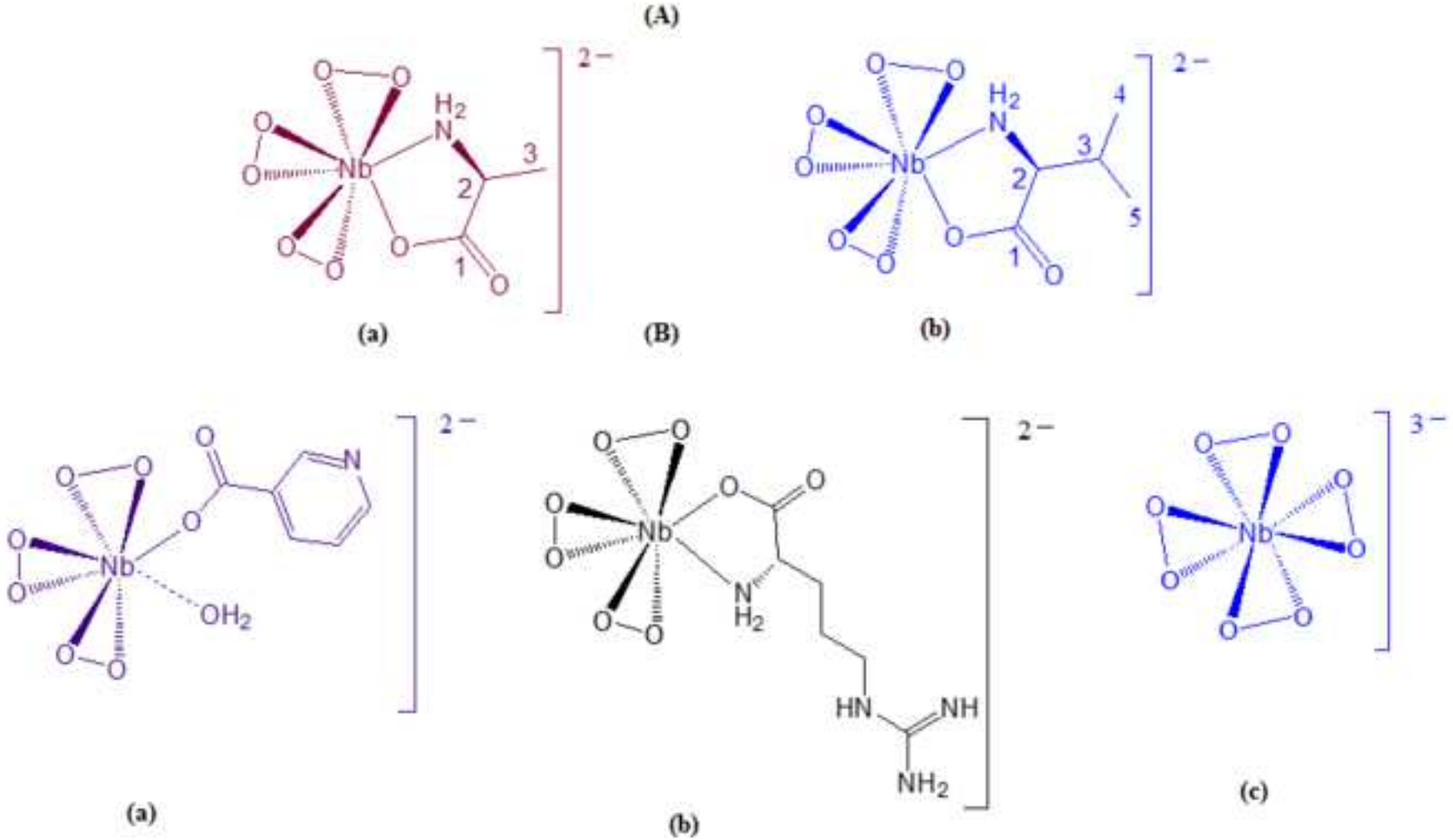

Fig. 5

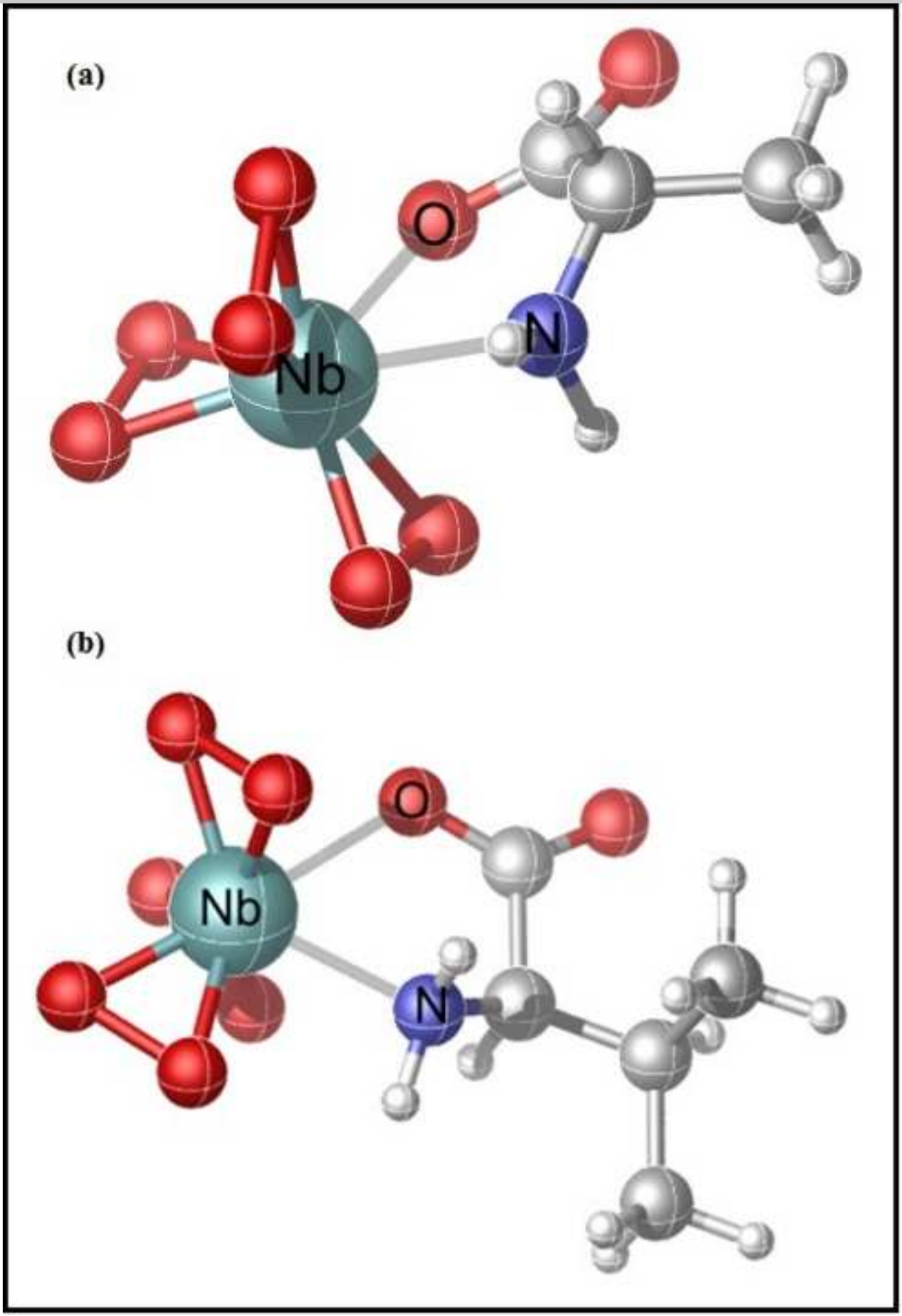

Fig. 6

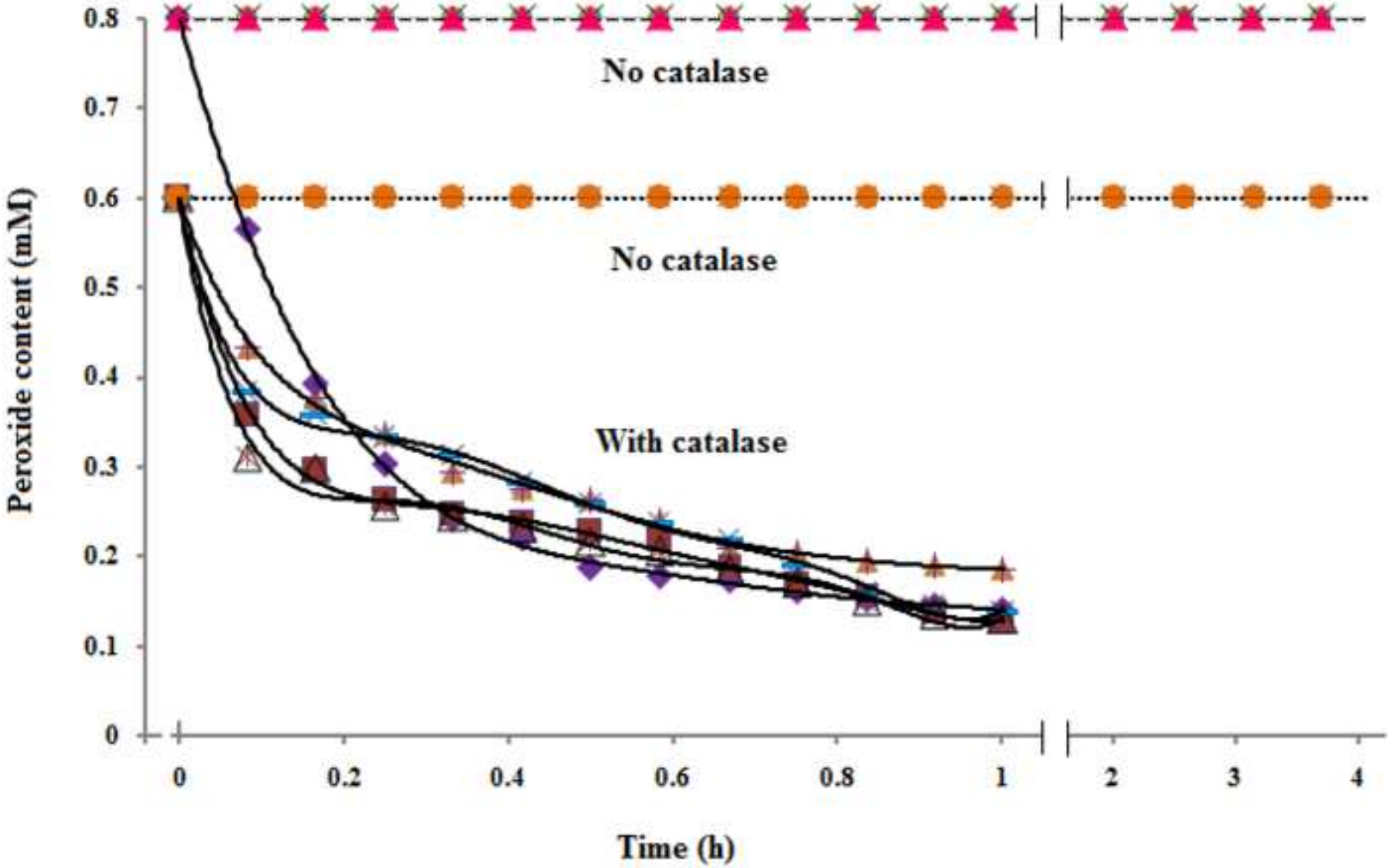

Fig. 7

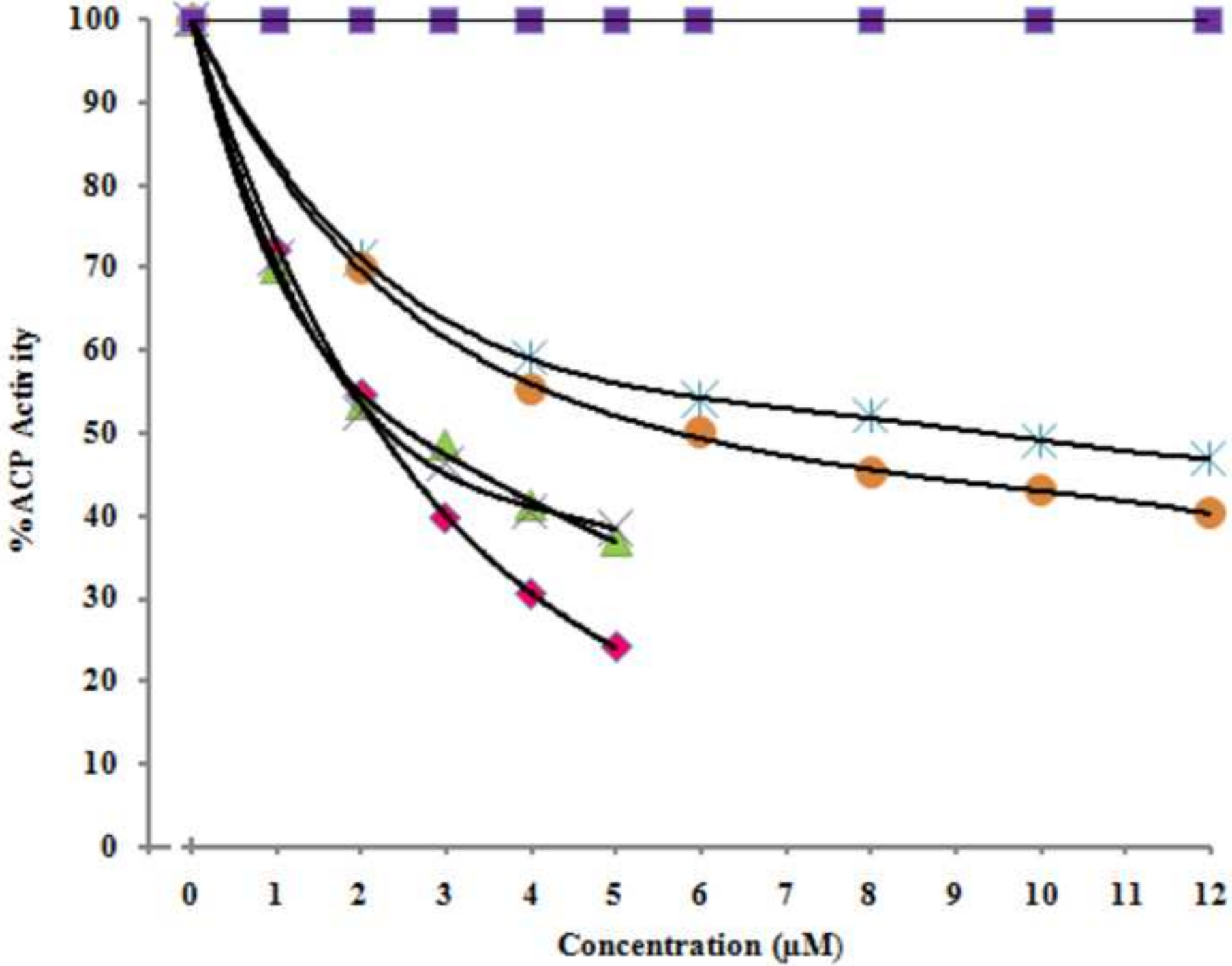

Fig. 8

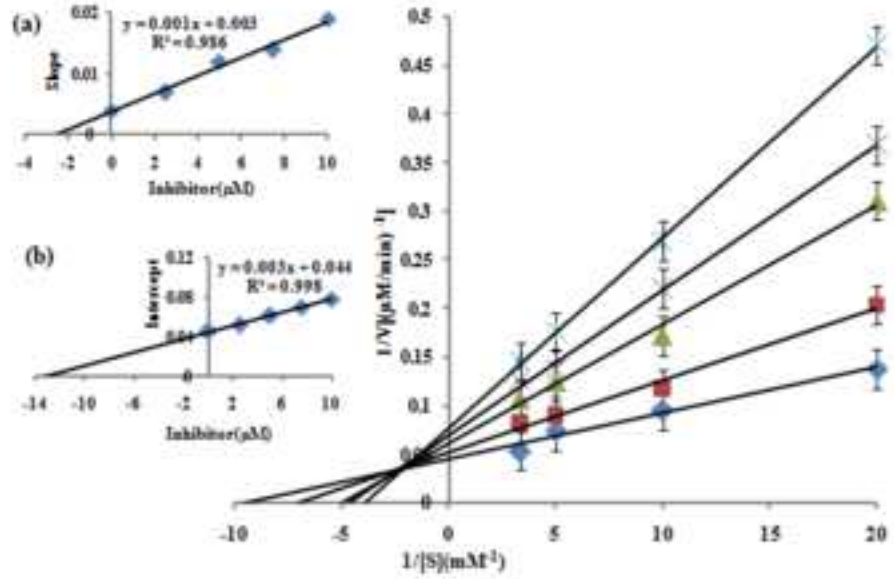

(A)

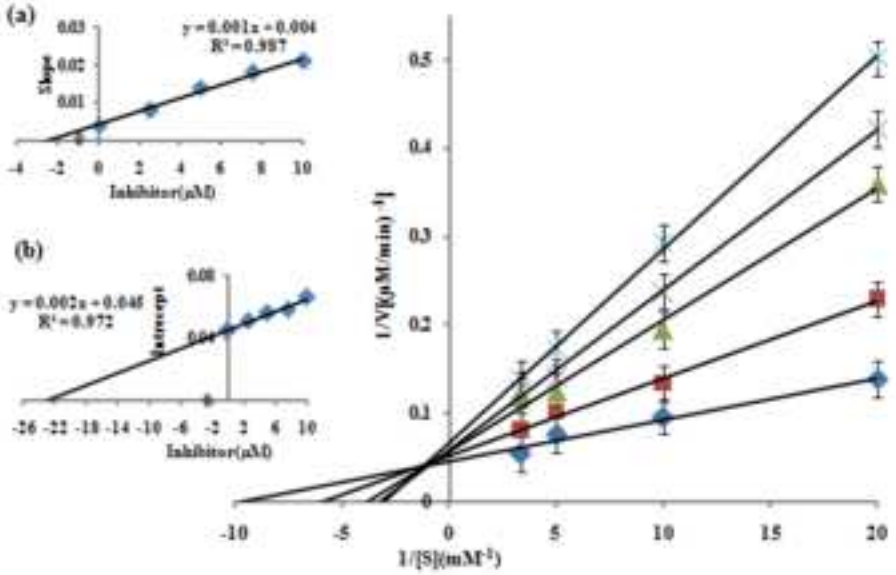

(B)

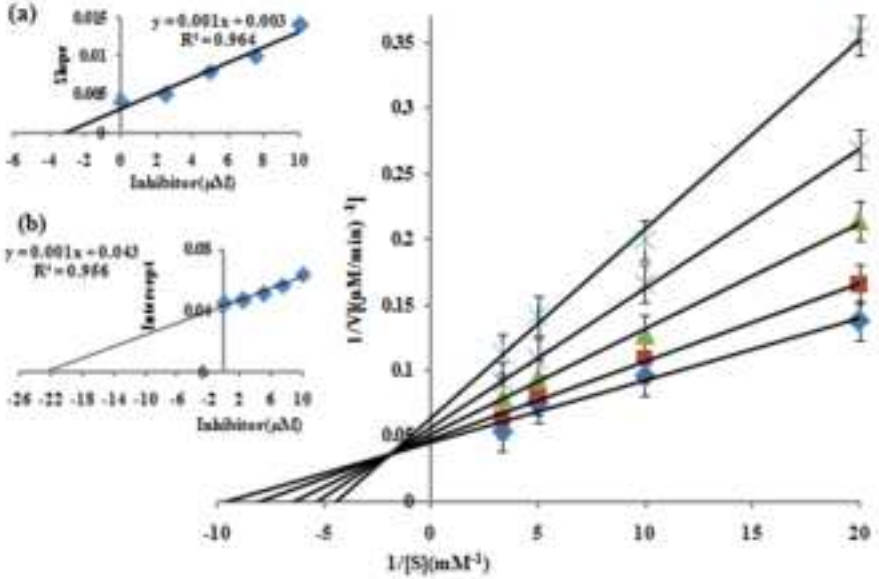

(C)

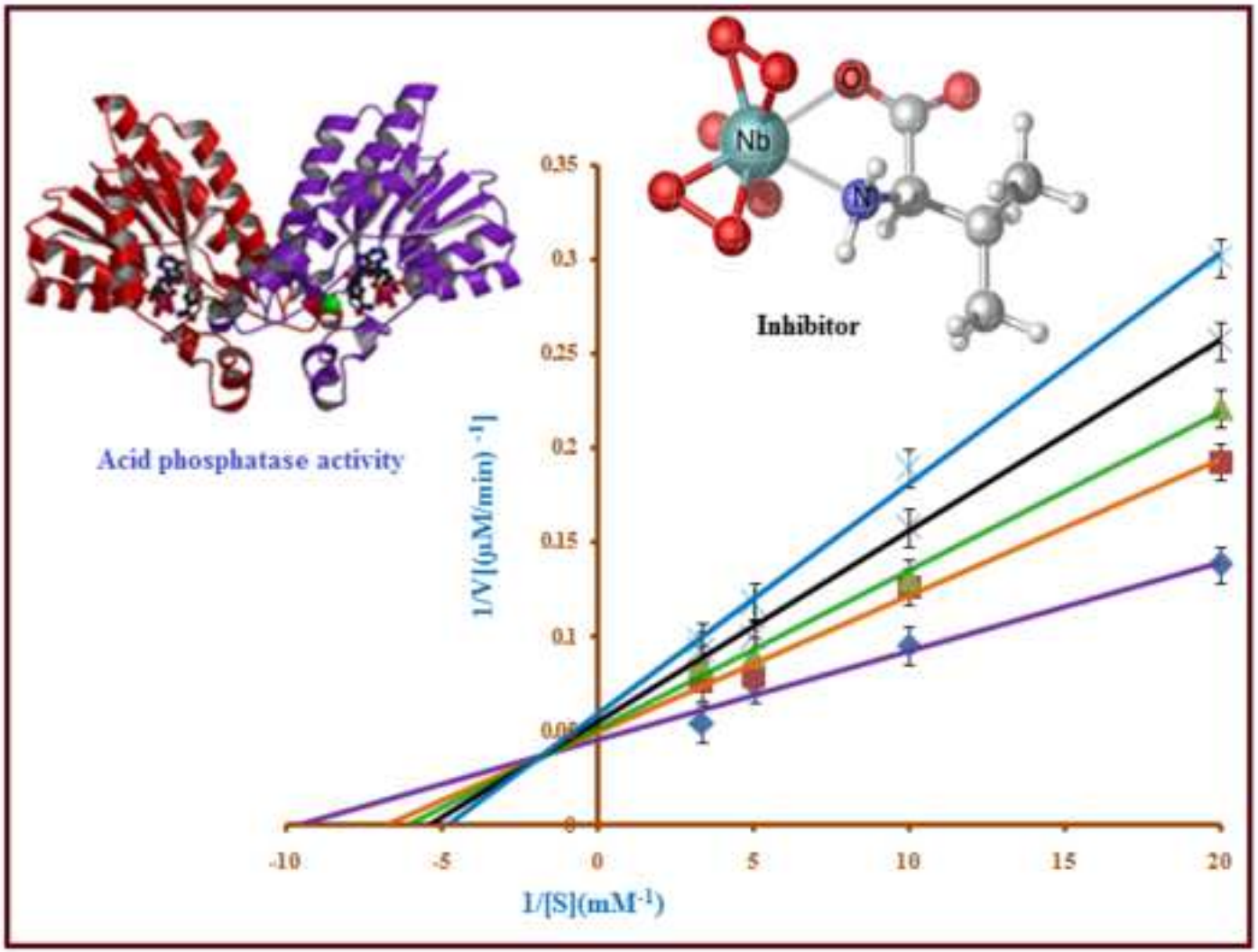

Graphical Abstract

Niobium(V) peroxo α-amino acid complexes: synthesis, stability and kinetics of inhibition of acid phosphatase activity

Sandhya Rani Gogoi, Gangutri Saikia, Kabirun Ahmed, Rituparna Duarah and Nashreen S. Islam*

Department of Chemical Sciences, Tezpur University, Tezpur 784028, Assam, India
E-mail: nsi@tezu.ernet.in
nashreen.islam@rediffmail.com

New heteroleptic triperoxoniobium complexes were synthesized, characterized and screened for their activities with the enzymes, catalase and acid phosphatase. The compounds retain their structural integrity in solution of pH ranging from 1.2-10, exhibit resistance to catalase action *vis-a vis* H_2O_2 and are potent mixed type of inhibitors of phosphatase.

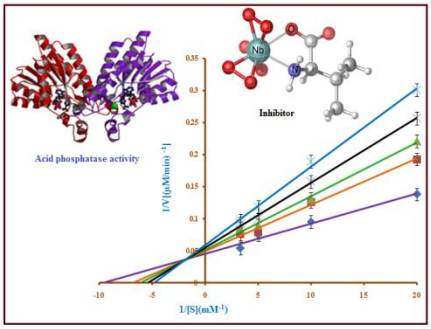

Niobium(V) peroxo α-amino acid complexes: synthesis, stability and kinetics of inhibition of acid phosphatase activity

Entry	Author	Degree	Designation	Email	Address
1.	Sandhya Rani Gogoi	M. Sc.	Research Scholar	sandhya@tezu.ernet.in	Dept. of Chemical Sciences, Tezpur University
2.	Gangutri Saikia	M. Sc.	Research Scholar	gsaikia@tezu.ernet.in	Dept. of Chemical Sciences, Tezpur University
3.	Kabirun Ahmed	M. Sc.	Research Scholar	kabirun@tezu.ernet.in	Dept. of Chemical Sciences, Tezpur University
4.	Rituparna Duarah	M. Sc.	Research Scholar	rituparnaduarah@gmail.com	Dept. of Chemical Sciences, Tezpur University